Taylor & Francis
Taylor & Francis Group

Determination of the radiation dose rate and radiogenic heat production of North Gabal Abu Hibban area, central Eastern Desert, Egypt

Mohamed Elsadek M. Sabra[a], Abdelaziz L. Abdeldayem[b], Mohamed A. S. Youssef[c], Alaa A. Masoud[b] and Salah A. Mansour[a]

[a]Egyptian Mineral Resources Authority, Cairo, Egypt; [b]Geology Department, Faculty of Science, Tanta University, Tanta, Egypt; [c]Exploration Division, Nuclear Materials Authority, Cairo, Egypt

ABSTRACT

Airborne gamma-ray spectrometric data for Gabal Abu Hibban area, central Eastern Desert, Egypt have been used for assessment of the radiation dose rate and recognize radiogenic heat production (RHP). The radioelement concentrations of eU (ppm), eTh (ppm) and K (%) were used to ascertain such rates for the rock units. Results showed several levels of radiation as follow; (less than 0.50 mSv/yr), (from 0.50 to 0.70 mSv/yr) and (from 0.70 to 2.5 mSv/yr). The dose rate more than 1 mSv/yr is considered the radioactivity hazard level which represented mainly with Mu'tiq group, Younger granite, Trachyte rocks and Duwi Formation. RHP calculations have been carried out for the various rock units to locate the highest radiogenic heat production. The rock units that possess relatively huge RHP are Mutiq group, Younger granite and Trachyte rocks with values more than 3 µWm^{-3}.

1. Introduction

Gamma-ray spectrometric maps are essential to define the contamination and prospecting to crude materials (in case of potassium alteration). Since field-based radiometric surveys need long-run consuming, airborne surveys are fast assessment method for expansive zones. Provision of airborne gamma-ray spectrometric (AGS) information has been intensively investigated by many researchers (Darnely 1973; Grasty 1987; Elkhadragy et al. 2016).

The studied area is located between longitudes 33° 50′ 42″ and 34° 21′ 09″ East, and latitudes 25° 54′ 13″ and 26° 15′ 27″ North, Central Eastern Desert (Figure 1). Airborne gamma-ray spectrometric surveys can determine the radioactive anomalous zones and concentration of the causative radioisotopes. The importance of this study is regarding to: a) The investigated area is subjected to a fast developments, therefore homes and groundwater wells must be away from highly radioactive zones. b) Radiogenic heat production must determine for each rock unit in the studied area.

2. Geologic setting

The exposed rock units and the observed structures of the studied area are shown in Figure 2. The litho-stratigraphy is explained by different sources such as Conoco (1987), EGSMA (1992) and EMRA (2009) into: A) Late Proterozoic rocks, started with Mu'tiq group, Ophiolite group, Hammamat clastics, Younger granite (calc alkaline of weakly deformed granitic rocks and alkaline undeformed granitic rocks), Dokhan volcanics, Post Hammamat and trachyte rocks. B) Cretaceous rocks, comprising three various units, from older to younger; Taref Formation, Quseir Formation and Duwi Formation. C) Cenozoic rocks, covered most northern and eastern parts of the area and represented by Tarawan Formation, Thebes Formation, Nakhil Formation, Umm Mahara and Ranga Formations, Umm Gheig and Abu Dabbab Formations, Shajara Formation and Quaternary deposits.

3. Data acquisition

Mineral, petroleum and groundwater assessment project (MPGAP) was performed as an airborne magnetic and spectrometric survey over immense piece of the Eastern Desert (Aero-Service. 1984). Flight path of this project (Figure 3) formed by parallel traverse lines with 1 km spacing and perpendicular tie lines with 10 km and mean terrain clearance about 120 m.

4. Data analysis and interpretation

Gamma-ray spectrometric analysis data of the area consist of the following stages:

(1) Separation of the radioelements over each lithologic unit
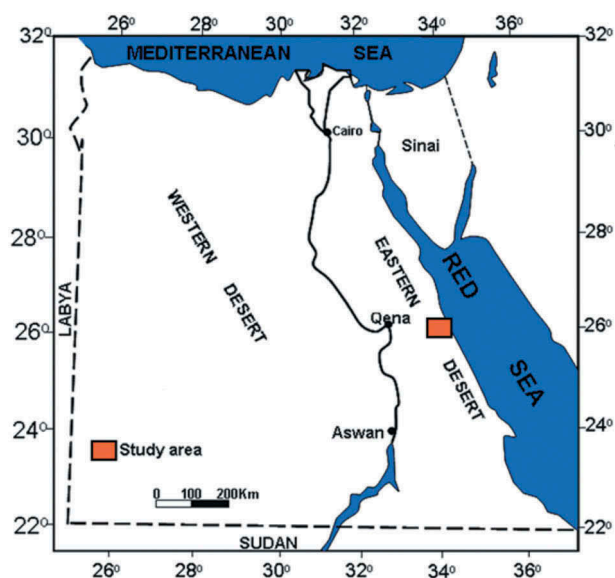(2) Determination of the characteristic statistics of these units, such as arithmetic mean (X),

Figure 1. Location map of north Gabal Abu Hibban area, central Eastern Desert, Egypt.
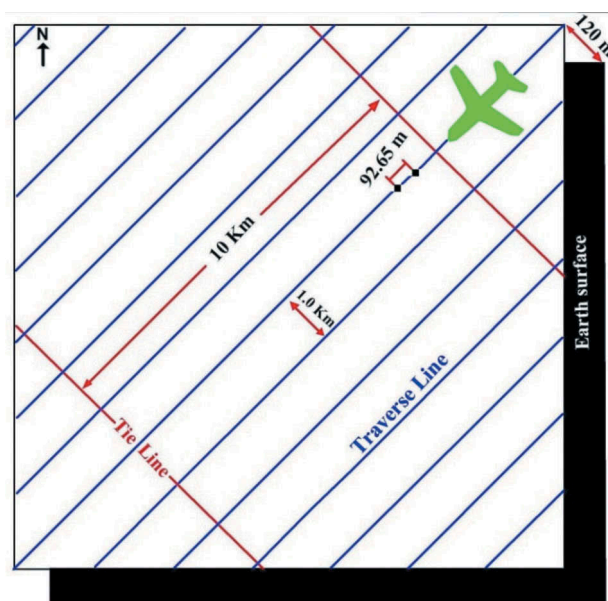

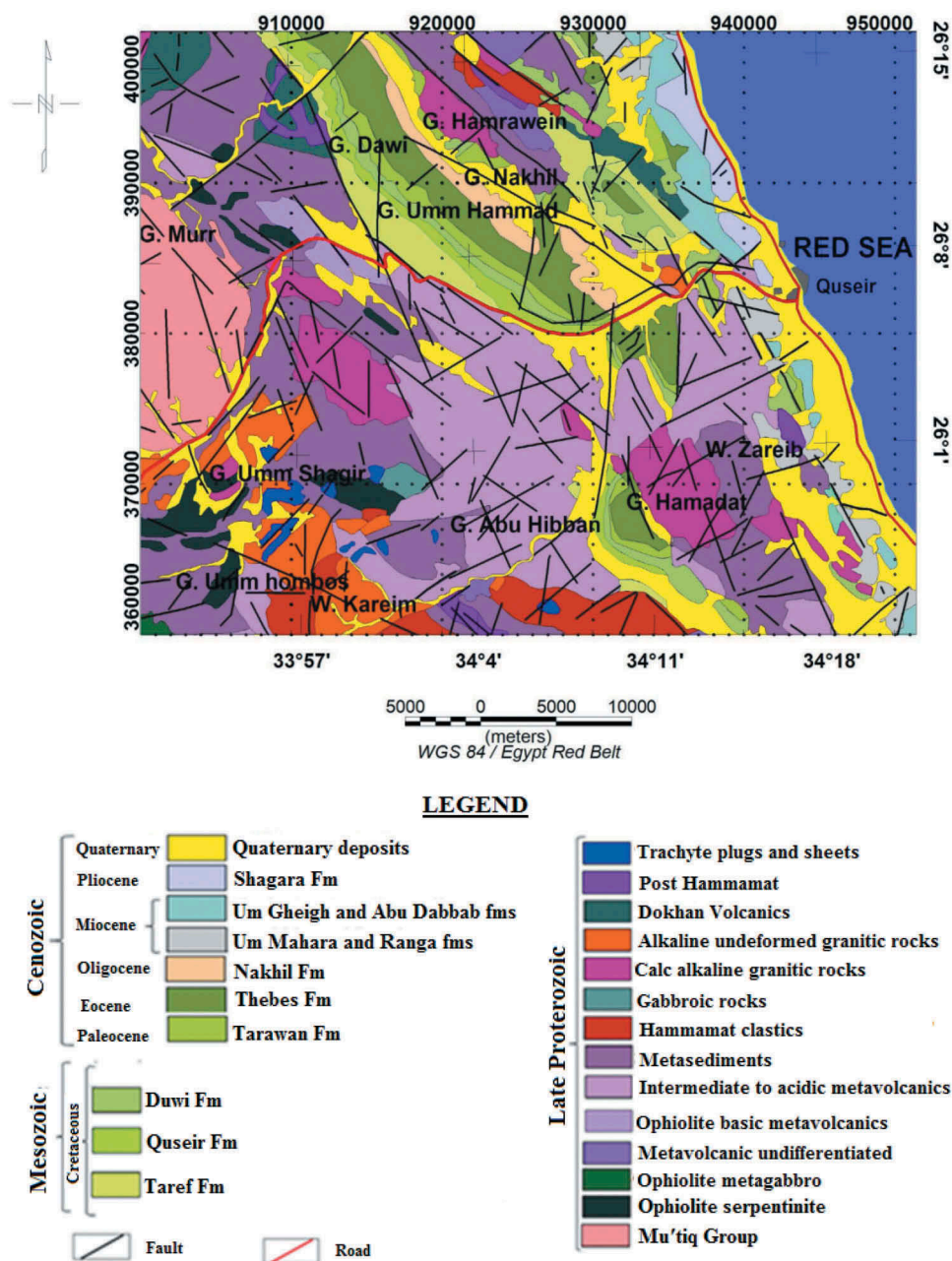**Figure 3.** Flight path of the MPGAP Project (Aero-Service. 1984).

LEGEND

Cenozoic		
Quaternary		Quaternary deposits
Pliocene		Shagara Fm
Miocene		Um Gheigh and Abu Dabbab fms
		Um Mahara and Ranga fms
Oligocene		Nakhil Fm
Eocene		Thebes Fm
Paleocene		Tarawan Fm

Mesozoic	Cretaceous	
		Duwi Fm
		Quseir Fm
		Taref Fm

Fault   Road

Late Proterozoic	
	Trachyte plugs and sheets
	Post Hammamat
	Dokhan Volcanics
	Alkaline undeformed granitic rocks
	Calc alkaline granitic rocks
	Gabbroic rocks
	Hammamat clastics
	Metasediments
	Intermediate to acidic metavolcanics
	Ophiolite basic metavolcanics
	Metavolcanic undifferentiated
	Ophiolite metagabbro
	Ophiolite serpentinite
	Mu'tiq Group

Figure 2. Geologic map of north Gabal Abu Hibban area, central Eastern Desert, Egypt. (Conoco 1987).

Table 1. Statistical analysis of (eU, eTh and K) variables in the basement rock units of north Gabal Abu Hibban area, central Eastern Desert, Egypt.

Age	Rock unit	Radioelements	Min	Max	X	SD	CV (%)
Precambrian	Trachyte plugs and sheets	T.C (µR/h)	24	130	68.8	28.8	41.8
		eU (ppm)	2.2	10.9	5.74	1.93	33.7
		eTh (ppm)	5.5	35.7	16.4	8.4	51.1
		K (%)	1.6	6.6	3.72	1.35	36.3
	Post Hammamat	T.C (µR/h)	26	94	58.02	16.54	28.5
		eU (ppm)	2.82	9	6.43	1.53	23.8
		eTh (ppm)	2.26	20.35	10.95	3.86	35.3
		K (%)	0.55	5.42	3.35	0.82	24.5
	Dokhan Volcanics	T.C (µR/h)	4	90	51.9	17.4	33.5
		eU (ppm)	0.74	19.9	8.01	3.59	44.7
		eTh (ppm)	0.89	16.7	8.55	3.25	38
		K (%)	0.22	5.7	2.23	1.26	56.7
	Alkaline undeformed granitic rocks	T.C (µR/h)	18	114	56.6	18.35	32.4
		eU (ppm)	1.64	9.8	5.13	1.31	25.5
		eTh (ppm)	3.3	26.5	11.8	4.41	37.4
		K (%)	1.06	5.5	3.2	0.94	29.4
	Calc alkaline of weakly deformed granitic rocks	T.C (µR/h)	14	140	73.84	34.93	47.3
		eU (ppm)	1.09	16.4	6.04	2.52	41.7
		eTh (ppm)	2.4	40.3	16.31	9.97	61.1
		K (%)	0.73	7.25	4.21	1.67	39.6
	Gabbroic Rocks	T.C (µR/h)	16	60	29.8	12.7	42.6
		eU (ppm)	1.2	7.7	3.4	1.79	52.5
		eTh (ppm)	3.6	16.3	7.1	3.25	45.7
		K (%)	0.99	2.9	1.79	0.54	30.1
	Hammamat Clastics	T.C (µR/h)	14	94	45.9	14.2	30.8
		eU (ppm)	1.5	9.1	5.04	1.32	26.2
		eTh (ppm)	2.6	24.01	9.4	3.43	36.3
		K (%)	0.8	5.2	2.5	0.66	26.1
	Metasediments	T.C (µR/h)	6	36	725.	7.5	29.3
		eU (ppm)	0.53	4.3	2.8	0.9	30.8
		eTh (ppm)	1.5	6.7	4.7	1.2	25.2
		K (%)	0.3	1.9	1.3	0.4	28.7
	Intermediate to Acidic metavolcanics	T.C (µR/h)	8	36	25.9	7.1	27.4
		eU (ppm)	0.8	4.9	3.3	1	0.43
		eTh (ppm)	1.6	7.2	5.1	1.3	25.5
		K (%)	0.3	2.2	1.5	0.4	29.3
	Basic Metavolcanics	T.C (µR/h)	12	58	36.9	13.96	37.9
		eU (ppm)	0.77	6.2	3.36	1.26	37.4
		eTh (ppm)	2.6	12.4	7.62	2.88	37.8
		K (%)	0.58	3.54	2.22	0.87	39.1
	Metavolcanic undifferentiated	T.C (µR/h)	26	58	43.7	12.3	28.2
		eU (ppm)	2.3	4.6	3.5	0.6	18
		eTh (ppm)	6.6	11.5	9.9	1.2	11.6
		K (%)	0.9	2.9	1.9	0.7	33.6
	Metagabbro	T.C (µR/h)	12	22	15.48	2.25	14.5
		eU (ppm)	1.67	3.04	2.18	0.42	19.2
		eTh (ppm)	3.92	4.04	3.99	0.02	0.5
		K (%)	0.54	1.17	0.79	0.14	18.8
	Serpentinite	T.C (µR/h)	4	28	17.2	6.7	39.1
		eU (ppm)	0.8	3.5	2.1	0.7	31.9
		eTh (ppm)	1.05	5.9	3.5	1.3	38.6
		K (%)	0.2	1.6	0.9	0.4	39.8
	Mu'tiq group	T.C (µR/h)	58	130	98.37	14.73	14.9
		eU (ppm)	4.3	14.5	9.28	1.84	19.9
		eTh (ppm)	9.7	27.3	18.7	3.43	18.3
		K (%)	3.41	7.02	5.75	0.61	10.7

where: **Min** = Minimum & **Max** = Maximum, **X** = Arithmetic mean, **SD** = Standard deviation, **CV %** = Coefficient of variability, **T.C** = Total count in µR/h, **eU** = Equivalent Uranium in (ppm), **eTh** = Equivalent Thorium in (ppm), **K** = potassium in (%), **µR/h** = Microroentgen per hour, ppm = Part of radioactive material per million pares of rock, **%** = Percent

standard deviation (SD), as well as checking the normality of distribution of all measurements was conducted using the coefficient of variation (Tables 1 and 2).

(3) Environmental impact computed by known radioelement variables for each lithological unit. The radiation exposure rate and dose rate were calculated and mapped.

(4) Calculation of RHP for all rock units.

4.1. Radioelements contour maps

The equivalent Uranium (eU in ppm) contour map (Figure 4) shows three different levels of uranium concentration values. The highest level (more than 6 ppm) is correlated mainly with Mu'tiq group in the western parts, as well as the Calc alkaline of weakly deformed granitic rocks in the SE parts of the area and huge NW belt of Duwi Formation.

Table 2. Statistical analysis of (eU, eTh and K) variables in the phanerozoic rock units of north Gabal Abu Hibban area, central Eastern Desert, Egypt.

Age	Rock unit	Radioelements	Min	Max	X	SD	CV (%)
Cenozoic	Quaternary	T.C (μR/h)	0.7	17.1	5.04	2.7	54.1
	Deposits	eU (ppm)	0.7	5.5	3.4	1.2	36.6
		eTh (ppm)	0.5	7.7	4.7	1.7	36.3
		K (%)	0.2	2.3	1.3	0.5	42.6
	Shajara	T.C (μR/h)	2	16	11.5	4.17	36.2
	Formation	eU (ppm)	0.98	3.23	2.26	0.53	23.6
		eTh (ppm)	1.2	2.78	1.92	0.31	16.2
		K (%)	0.19	2.5	0.69	0.65	95
	Um Gheigh and Abu	T.C (μR/h)	4	50	18.1	9.78	54.1
	Dabbab formations	eU (ppm)	0.65	8.24	2.67	1.63	60.9
		eTh (ppm)	0.57	8.39	2.42	1.67	69.1
		K (%)	0.18	2.01	0.63	0.42	66.3
	Um Mahara	T.C (μR/h)	0.7	11.8	5.05	3.2	64
	and Ranga	eU (ppm)	0.7	5.04	2.9	1.1	40.2
	formations	eTh (ppm)	1.4	5.9	3.9	1.3	32.7
		K (%)	0.2	1.7	1	0.3	34.8
	Nakhil	T.C (μR/h)	14	46	32.4	7.2	22.2
	Formation	eU (ppm)	2.4	6.9	5.2	1.05	20.3
		eTh (ppm)	1.5	5.8	3.7	1.1	29.3
		K (%)	0.4	2.2	1.2	0.5	42
	Thebes	T.C (μR/h)	6	36	26.3	5.9	22.7
	Formation	eU (ppm)	0.7	7.5	5.6	1.3	24
		eTh (ppm)	0.9	4.6	2.9	0.9	30.3
		K (%)	0.2	1.6	0.9	0.3	34.2
	Tarawan	T.C (μR/h)	12	36	26.6	5.9	22.4
	Formation	eU (ppm)	1	7.6	5.1	1.7	33.8
		eTh (ppm)	1.8	4.7	2.8	0.8	29
		K (%)	0.3	1.9	0.9	0.4	41.9
Mesozoic	Duwi	T.C (μR/h)	8	80	38.5	14.42	37.4
	Formation	eU (ppm)	1.8	18.7	8.6	3.58	41.5
		eTh (ppm)	1.32	12.4	4.68	2.52	53.8
		K (%)	0.29	4.2	1.66	0.93	56.1
	Quseir	T.C (μR/h)	6	42	29. 6	9.1	30. 7
	Formation	eU (ppm)	1.1	9.9	6.2	2.3	37.4
		eTh (ppm)	1.5	5.9	3.4	1.1	32.3
		K (%)	0.22	2	1.1	0.5	43.9
	Taref	T.C (μR/h)	18	46	34.1	8.5	24.9
	Formation	eU (ppm)	1.7	11.9	7.7	2.8	35.9
		eTh (ppm)	1.7	5.8	4.1	0.9	23.9
		K (%)	0.4	2.9	1.4	0.5	39.1

where: **Min** = Minimum & **Max** = Maximum, **X** = Arithmetic mean, **SD** = Standard deviation, **CV %** = Coefficient of variability, **T.C** = Total count in μR/h, **eU** = Equivalent Uranium in (ppm), **eTh** = Equivalent Thorium in (ppm), **K** = potassium in (%), **μR/h** = Microroentgen per hour, **ppm** = Part of radioactive material per million pares of rock, **%** = Percent.
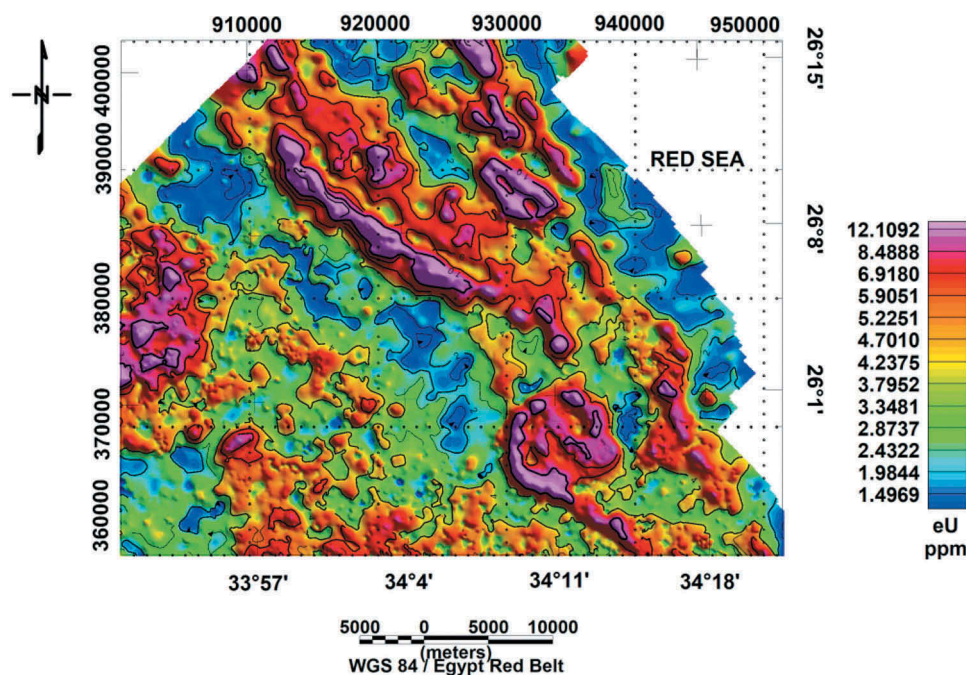
Figure 4. Fill coloured contour map of equivalent Uranium (eU) in ppm, north Gabal Abu Hibban area, central Eastern Desert, Egypt.
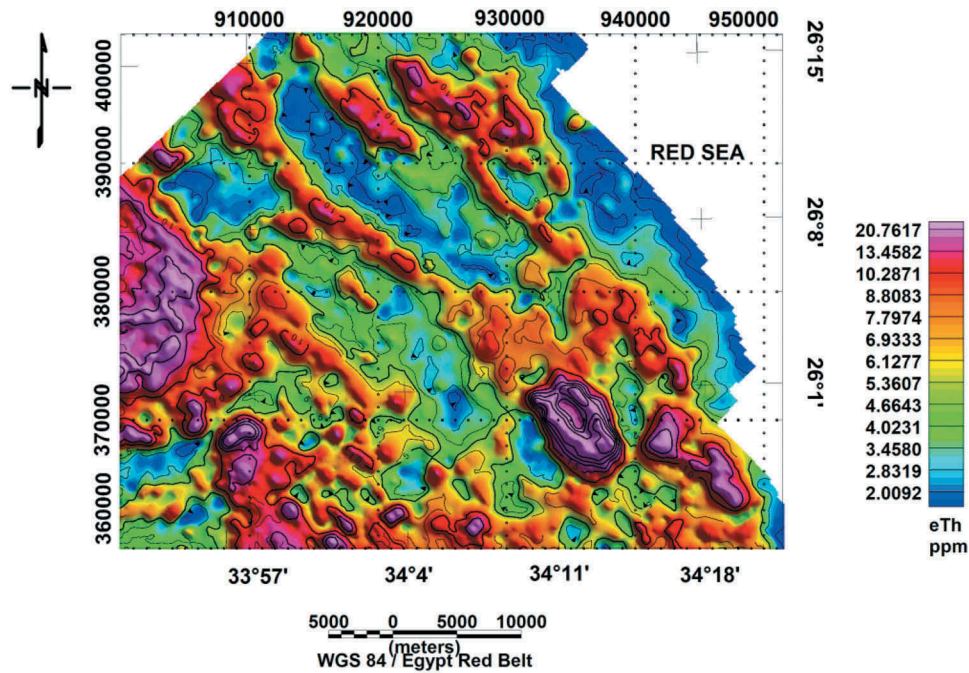
Figure 5. Fill coloured contour map of equivalent Thorium (eTh) in ppm, north Gabal Abu Hibban area, central Eastern Desert, Egypt.

The intermediate level ranged from 3.5 to 6 ppm and associated mainly with Hammamat Clastics. The lowest level is less than 3.5 ppm and associated with the Intermediate to acidic metavolcanics, Metasediments, Um Gheigh and Abu Dabbab formations and Shajara Formation.

The equivalent thorium (eTh in ppm) contour map (Figure 5) is divided into three levels of thorium concentrations. The lowest level associated mainly with Thebes Formation, Um Gheigh and Abu Dabbab formations, Shajara Formation and

Quaternary Deposits and having values less than 5 ppm. The intermediate level ranged from 5 to 7 ppm and recorded over Intermediate to acidic metavolcanics. The highest level (more than 7 ppm) is related to Mu'tiq group and Younger granite.

Figure 6 shows the potassium contour map, (K in %). The values of potassium concentrations can be divided into three levels of concentrations. The lowest level (less than 1.5%) is associated with Intermediate to acidic metavolcanics, Thebes
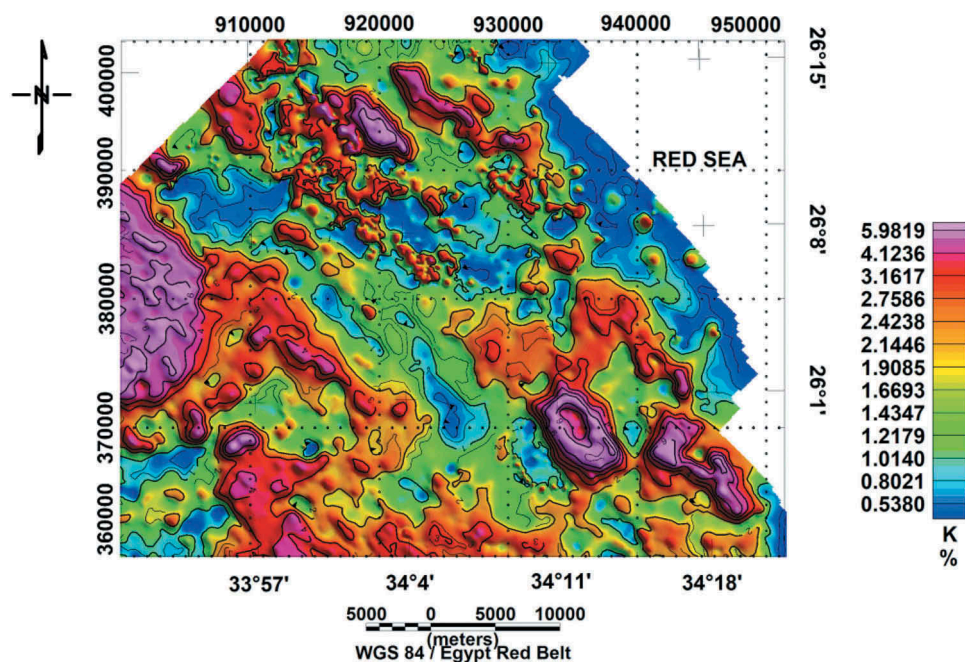

Figure 6. Fill coloured contour map of Potassium (K) in %, north Gabal Abu Hibban area, central Eastern Desert, Egypt.

Formation, Um Mahara and Ranga formations, Um Gheigh and Abu Dabbab formations, Shajara Formation and Quaternary Deposits. The values ranging from (1.5–2.2%) are represented the intermediate level and associated with Hammamat clastics. The third level is the highest zone (more than 2.2%) and is recorded over Mu'tiq group, younger granite and Dokhan Volcanics of the studied area.

4.2. Environmental impacts

The radiation exposure rate was calculated by applying the following expression (IAEA 1991):

$$\textbf{Exposure rate } (\mu\textbf{Rhr}^{-1}) = \textbf{1}.505\textbf{K (percent)} \\ + \textbf{0.653 eU (ppm)} \\ + \textbf{0.287 eTh (ppm)}$$
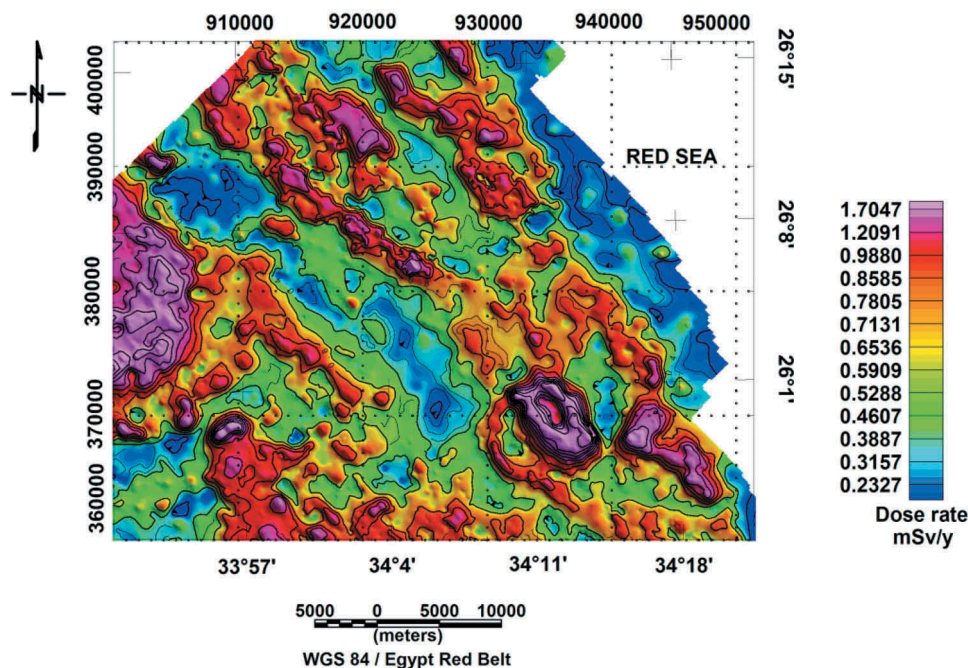

Figure 7. Radiation dose rate colour map of north Gabal Abu Hibban area, central Eastern Desert, Egypt.

Table 3. Radiation dose rates in mSv/y for the different rock units of north Gabal Abu Hibban area, central Eastern Desert, Egypt.

Age	Rock Units	Dose rate (mSv/y)			
		Min	Max	X	SD
Cenozoic	Quaternary Deposits	0.08	0.7	0.4	0.14
	Shajara Formation	0.13	0.56	0.27	0.13
	Um Gheigh and Abu Dabbab formations	0.08	0.67	0.28	0.51
	Um Mahara and Ranga formations	0.15	0.5	0.3	0.1
	Nakhil Formation	0.05	0.7	0.3	0.2
	Thebes Formation	0.1	0.7	0.3	0.15
	Tarawan Formation	0.1	0.6	0.3	0.1
Mesozoic	Duwi Formation	0.20	1.42	0.79	0.23
	Quseir Formation	0.1	0.9	0.4	0.18
	Taref Formation	0.1	1	0.4	0.2
Precambrian	Trachyte plugs and sheets	0.48	2.2	1.17	0.45
	Post Hammamat	0.5	1.53	1.03	0.21
	Dokhan Volcanics	0.1	1.6	0.92	0.25
	Alkaline undeformed granitic rocks	0.35	1.8	0.96	0.26
	Calc alkaline of weakly deformed granitic rocks	0.24	2.5	1.24	0.55
	Gabbroic rocks	0.28	1.1	0.58	0.23
	Hammamat clastics	0.29	1.5	0.81	0.21
	Metasediments	0.1	0.6	0.4	0.1
	Intermediate to acidic metavolcanics	0.1	0.7	0.4	0.11
	Basic metavolcanics	0.19	0.99	0.64	0.23
	Metavolcanic undifferentiated	0.2	0.7	0.5	0.1
	Metagabbro	0.26	0.38	0.31	0.03
	Serpentinite	0.1	0.5	0.3	0.1
	Mu'tiq group	0.99	2.2	1.67	0.22

Where: X = Arithmetic mean. SD = Standard deviation.

The radiation exposure rate can be converted to equivalent radiation dose rate (RDR) as follows (IAEA 1979):

Dose rate $(\mathbf{mSv\ yr^{-1}}) = \mathbf{0.0833_*}$ exposure rate$(\mathbf{\mu Rhr^{-1}})$

The RDR map can be subdivided into three levels (Figure 7 and Table 3). The lowest level having values less than 0.50 mSv/y. This level is associated with the Serpentinite, Tarawan Formation as well as Um Mahara and Ranga formations and Shajara Formation. The second level is the intermediate level, which ranges between 0.50 to 0.70 mSv/y and is associated with Tarawan, Thebes, Nakhil formations, Intermediate to acidic metavolcanics and Metasediments.

The highest level (radioactivity hazard level) has values over than 0.70 mSv/y and is recorded in the Mu'tiq group, Younger granit, Trachyte plugs and sheets and Duwi Formation. The highest value related to Calc alkaline of weakly deformed granitic rocks and reached to 2.5 mSv/y. The International Commission of Radiological Protection (ICRP) has recommended that, no individual should receive more than one millisievert per year (IAEA, 2000).

4.3. Radiogenic heat production (RHP)

Radiogenic heat producing rocks are often targets for geothermal exploration and production (McCay et al. 2014). Rybach (1976) published an empirical equation to calculate the RHP of a given rock sample using the following equation.

$$\mathbf{RHP}\ \left[\mathbf{\mu W/m^3}\right] = \rho * \begin{pmatrix} \mathbf{0.0952\ CU} \\ +\mathbf{0.0256\ CTh} \\ +\mathbf{0.0348\ CK} \end{pmatrix}$$

Where: ρ is the dry density of the rock (g/cm³) while, CU, CT hand CK are the concentrations of U and Th in ppm and K in %, respectively. The constants 0.0952, 0.0256 and 0.0348 are the radiogenic heat generation rate per mass of eU, eTh and K, respectively (Rybach 1988).

The average densities for each rock unit are shown in Table 4. Figure 8 represents the radiogenic heat production colour map of the study area, and statistical characteristics of RHP (mean and standard deviation) are shown in Table 5.

The area possesses a range of radioactive heat production varying from 0.05 to 6.9 μWm^{-3} using Rybach's (1976). The highest average values (Table 5) are obtained for Calc alkaline of weakly deformed granitic rocks and Mu'tiq group (6.9 μWm^{-3}) and (6.2 μWm^{-3}), respectively, whereas the lowest average values are obtained for Metasediments and Quaternary deposits (0.05 μWm^{-3}).

Arithmetic mean of RHP values can be separated into three levels according to the previously mentioned method. The highest values over 1.8 μWm^{-3} associated mainly with Mu'tiq group, Younger granite, Trachyte plugs and sheets and Duwi Formation that can be a targeted for geothermal resource exploration. The intermediate average RHP values are recorded in areas over Basic metavolcanics, Intermediate to acidic metavolcanics, Gabbroic rocks and Taref Formation with values ranging

Table 4. Average density for each rock unit in the study area (Website: http://geopixel.co.uk/lab3/Densities_of_Typical_Rock_Types_and_Minerals.pdf).

| Age	Rock Units	Average Density (g/cm³)
Cenozoic	Quaternary Deposits	1.92
	Shajara Formation	2.50
	Um Gheigh and Abu Dabbab formations	2.22
	Um Mahara and Ranga formations	2.50
	Nakhil Formation	2.0
	Thebes Formation	2.55
	Tarawan Formation	2.40
Mesozoic	Duwi Formation	2.50
	Quseir Formation	2.35
	Taref Formation	2.35
Precambrian	Trachyte plugs and sheets	2.80
	Post Hammamat	2.65
	Dokhan Volcanics	2.61
	Alkaline undeformed granitic rocks	2.64
	Calc alkaline of weakly deformed granitic rocks	2.64
	Gabbroic rocks	3.03
	Hammamat clastics	2.61
	Metasediments	2.62
	Intermediate to acidic metavolcanics	2.72
	Basic metavolcanics	2.78
	Metavolcanic undifferentiated	2.64
	Metagabbro	2.93
	Serpentinite	2.65
	Mu'tiq group	2.80
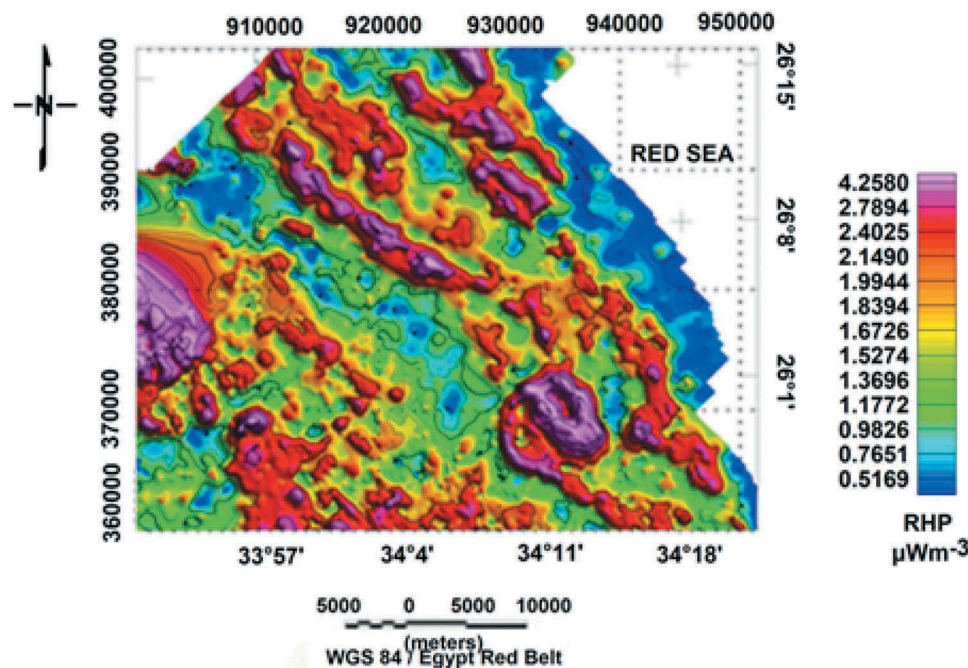
Figure 8. Radiogenic heat production colour map of north Gabal Abu Hibban area, central Eastern Desert, Egypt using Rybach (1976).

Table 5. Statistical calculations of radiogenic heat production rate corresponding to each rock unit (in μWm^{-3}) using Rybach's (1976) equation.

Age	Rock Units	Radiogenic Heat Production Rate (RHP) (μWm^{-3})			
		Min	Max	X	SD
Cenozoic	Quaternary Deposits	0.05	1.5	0.7	0.3
	Shajara Formation	0.36	0.93	0.72	0.15
	Um Gheigh and Abu Dabbab formations	0.21	1.98	0.75	0.40
	Um Mahara and Ranga formations	0.1	1.5	0.7	0.4
	Nakhil Formation	0.1	1.6	0.8	0.5
	Thebes Formation	0.1	2.2	0.8	0.7
	Tarawan Formation	0.1	2.01	0.7	0.6
Mesozoic	Duwi Formation	0.60	4.81	2.49	0.85
	Quseir Formation	0.1	2.7	0.9	0.8
	Taref Formation	0.1	3.1	1.1	0.9
Precambrian	Trachyte plugs and sheets	1.2	6.02	3.1	1.19
	Post Hammamat	1.37	3.7	2.67	0.59
	Dokhan Volcanics	0.26	5.39	2.76	0.86
	Alkaline undeformed granitic rocks	0.77	4.38	2.38	0.63
	Calc alkaline of weakly deformed granitic rocks	0.64	6.9	3.01	1.38
	Gabbroic rocks	0.76	3.7	1.72	0.78
	Hammamat clastics	0.73	4.02	2.11	0.55
	Metasediments	0.05	1.7	0.9	0.4
	Intermediate to acidic metavolcanics	0.1	1.97	1.1	0.4
	Basic metavolcanics	0.48	2.63	1.64	0.59
	Metavolcanic undifferentiated	0.7	1.8	1.4	0.3
	Metagabbro	0.82	1.24	0.98	0.12
	Serpentinite	0.1	1.3	0.7	0.3
	Mu'tiq group	2.5	6.2	4.37	0.71

Where: X = Arithmetic mean. SD = Standard deviation.

from 1 to 1.8 μWm^{-3}. The lowest average RHP values are obtained from Serpentinite, Metagabbro, Metasediments, Quseir Formation and Cenozoic rock units. In these areas, the RHP values are less than 1 μWm^{-3}.

5. Conclusions

The AGS data have been useful for assessing the environmental impact of the different rock units in north Gabal Hibban area, CED. Most of the rock units in the studied area are saved except highest level (with values over than 0.70 mSv/y), which correlated mainly with Mutiq group, Younger granite, Trachyte rocks and Dawi Formation. It is therefore recommended to stay away from these sites when planning to drill wells for groundwater or constructing new settlements in these sites. Mu'tiq group, Granitic rocks, Trachyte plugs and Duwi Formation can be used for geothermal resource exploration.

Disclosure statement

No potential conflict of interest was reported by the authors.

References

Aero-Service. 1984. Final operational report of airborne magnetic/radiation survey in the Eastern Desert, Egypt. For the Egyptian General Petroleum Corporation (EGPC) and the Egyptian Geological Survey and Mining Authority (EGSMA). Houston (Texas, USA): Aero-Service Division. Six Volumes.

Conoco. 1987. Geological map of Egypt, Scale (1:500,000), NG36 NE-Quseir sheet and NG 36 SE-Gebel Hamata sheet.

Darnely AG. 1973. Airborne gamma-ray survey techniques, present and future, in uranium exploration methods, proceeding of panel. Venna: International Atomic Energy Agency; p. 67–108.

EGSMA (Egyptian Geological Survey and Mining Authority). 1992. Geology of Al Quseir quadrangle. Egypt.

Elkhadragy AA, Abdelaziz AMS, Gharieb AGN, El-Husseiny AA. 2016. The use of airborne spectrometric data in geological mapping and uranium exploration at Qena-Quseir Shear Zone Area, Eastern Desert, Egypt. Global J Sci Front Res Environ Earth Sci. 16(5). Version 1. 21 pp.

EMRA. (Egyptian Mineral Resources Authority). 2009. Geology of Wadi Al Barramiyah quadrangle. Egypt.

Grasty RL. 1987. the design, construction and application of air borne gamma-ray spectrometer calibration pads. Geol Surv Can. 87–10:43.

IAEA. 1979. Gamma-ray surveys in uranium exploration. Technical Report Series, No. 186. Vienna (Austria): IAEA; 90pp.

IAEA. 1991. Airborne gamma-ray spectrometer surveying. Technical Report Series, No. 323, Vienna (Austria): IAEA; 97pp.

IAEA (International Atomic Energy Agency). 2000. 5th international conference on high level of natural radiation, Munich, 2000. Waste solutions. Vol.42 No3, Vienna (Austria), pp7.

McCay AT, Harley TL, Younger PL, Sanderson DCW, Cresswell AJ. 2014. Gamma-ray spectrometry in geothermal exploration: state of the art techniques. Energies. 7(8):4757–4780. doi:10.3390/en7084757.

Rybach L. 1976. Radioactive Heat production in rocks and its relation to other pertrophysical parameters, pure & appl. Geophysics. 114:309–318.

Rybach L. 1988. Determination of heat production rate. In R. Hänel, L. Rybach, L. Stegena, (eds.), Handbook of terrestrial heat flow density determination. Dordrecht: Kluwer; p. 125–142.